



Contents lists available at ScienceDirect

Nuclear Instruments and Methods in Physics Research A

journal homepage: www.elsevier.com/locate/nima

The CBM RICH project

J. Adamczewski-Musch^a, P. Akishin^h, K.-H. Becker^b, S. Belogurov^c, J. Bendarouach^d, N. Boldyreva^e, A. Chernogorov^c, C. Deveau^d, V. Dobyryn^e, M. Dürr^d, J. Eschke^a, J. Förtsch^b, J. Heep^d, C. Höhne^d, K.-H. Kampert^b, L. Kochenda^{e,f}, J. Kopfer^b, P. Kravtsov^{e,f}, I. Kres^b, S. Lebedev^{d,h}, E. Lebedeva^d, E. Leonova^e, S. Linev^a, T. Mahmoud^d, J. Michel^g, N. Miftakhov^e, W. Niebur^a, E. Ovcharenko^c, V. Patel^b, C. Pauly^{b,*}, D. Pfeifer^b, S. Querschfeld^b, J. Rautenberg^b, S. Reinecke^b, Y. Riabov^e, E. Roshchin^e, V. Samsonov^{e,f,i}, O. Tarasenkova^e, M. Traxler^a, C. Ugur^a, E. Vznuzdaev^e, M. Vznuzdaev^e

^a GSI Helmholtzzentrum für Schwerionenforschung GmbH, D-64291 Darmstadt, Germany^b Department of Physics, University of Wuppertal, D-42097 Wuppertal, Germany^c SSC RF ITP, 117218 Moscow, Russia^d Institute of Physics II and Institute of Applied Physics, Justus Liebig University Giessen, D-35392 Giessen, Germany^e National Research Centre "Kurchatov Institute" B.P. Konstantinov Petersburg Nuclear Physics Institute, 188300 Gatchina, Russia^f National Research Nuclear University MEPhI (Moscow Engineering Physics Institute), 115409 Moscow, Russia^g Institut für Kernphysik, Göthe University Frankfurt, D-60438 Frankfurt am Main, Germany^h Laboratory of Information Technologies, Joint Institute for Nuclear research (JINR-LIT), Dubna, Russiaⁱ St. Petersburg Polytechnic University (SPbPU), St. Petersburg, Russia

ARTICLE INFO

Article history:

Received 4 April 2016

Accepted 24 May 2016

Keywords:

Ring Imaging Cherenkov detector RICH
MAPMT

Radiation hardness

FPGA-TDC

Electronic readout

Detector

ABSTRACT

The CBM RICH detector is an integral component of the future CBM experiment at FAIR, providing efficient electron identification and pion suppression necessary for the measurement of rare dileptonic probes in heavy ion collisions. The RICH design is based on CO₂ gas as radiator, a segmented spherical glass focussing mirror with Al+MgF₂ reflective coating, and Multianode Photomultipliers for efficient Cherenkov photon detection. Hamamatsu H12700 MAPMTs have recently been selected as photon sensors, following an extensive sensor evaluation, including irradiation tests to ensure sufficient radiation hardness of the MAPMTs. A brief overview of the detector design and concept is given, results on the radiation hardness of the photon sensors are shown, and the development of a FPGA-TDC based readout chain is discussed.

© 2016 Elsevier B.V. All rights reserved.

1. The CBM experiment

The phase diagram of strongly interacting baryonic matter is a fascinating subject of modern research. In analogy to the well known phase diagram of ordinary matter, it describes the state or "phases" of baryonic matter as function of two thermodynamic state variables: The temperature, and the baryochemical potential (or net-baryon density). Moving up the temperature axis at low baryochemical potential, a smooth crossover from normal, hadronic, confined matter to a partonic state of matter known as the quark-gluon plasma is observed, where the quarks and gluons are no longer confined to hadrons. The intermediate region of this phase diagram is of particular interest, where matter is expected

to behave differently due to effects of the large net-baryon density. New phenomena are predicted by QCD, like the manifestation of a first-order phase transition from hadronic to partonic matter, including a critical endpoint separating the phase transition from the crossover at high temperature, or the partial restoration of chiral-symmetry close to the phase transition.

On earth, the only way to study matter at these extreme conditions experimentally is by means of heavy ion collisions. It is the primary aim of the future CBM experiment at FAIR in Darmstadt, Germany, to explore the high density and moderate temperature region of the phase diagram with unprecedented statistical accuracy (up to 10 MHz Au–Au interaction rate). Designed as a fixed target experiment, CBM will make use of the high intensity ion beams of the SIS100 accelerator, with energies up to 11 AGeV for the heaviest nuclei (up to 35 AGeV with the possible installation of the SIS300 accelerator in future). The measurement of dileptonic probes is one important aspect of the proposed experimental

* Corresponding author.

E-mail address: pauly@physik.uni-wuppertal.de (C. Pauly).

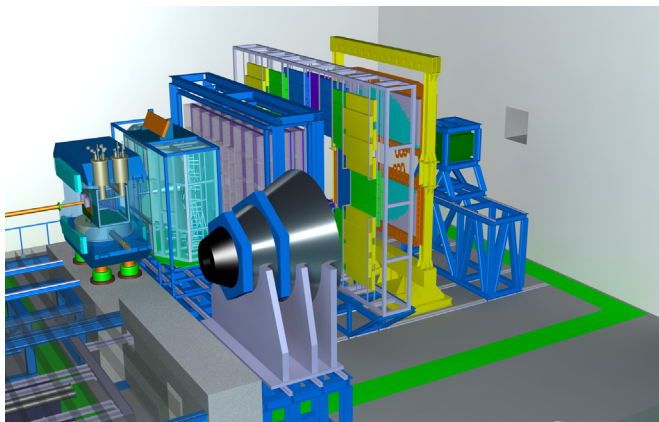


Fig. 1. The CBM detector setup showing from left to right: The CBM dipole with MVD and STS tracking system, RICH detector (Muon detection system in front), Transition Radiation detector (TRD), Time-of-Flight wall (ToF), Electromagnetic Calorimeter ECAL, and the projectile spectator detector (PSD) at the far right side.

program. Rare dileptonic decays of light vector mesons like the short-lived ρ ($\tau \approx 10^{-24}$ s, $\text{BR} \approx 10^{-4}$) are penetrating probes, providing access to the early, high-density phase of the collision process, undisturbed by secondary interactions with the dense, hadronic medium. They allow for example to study the in-medium properties of the ρ meson and effects of chiral restoration. A detailed overview of the CBM physics program is given in [1].

A sketch of the CBM detector setup (in its electron configuration) is shown in Fig. 1. Central component is a state-of-the-art silicon tracking system, consisting of 8 individual tracking layers of double-sided silicon strip-detectors inside the large super-conducting dipole magnet. The measurement of di-electron probes requires excellent particle identification, in particular e/π separation, which is achieved using a large Ring-Imaging Cherenkov detector, the CBM RICH. For measurement of di-muon probes, the RICH is interchanged with a large Muon detection system, also shown in Fig. 1. Particle reconstruction and tracking is further extended using a Micro Vertex Detector (MVD), Transition Radiation Detectors (TRD), a Time-of-Flight (ToF) detection system, an ECAL, and a Projectile Spectator Detector (PSD).

2. The CBM RICH detector

The CBM RICH detector (Fig. 2) is the main detection system for electron/pion separation for particle momenta up to ≈ 8 GeV/c, providing pion suppression factors well above 100. It uses a CO_2 gas radiator at 2 mbar overpressure ($\gamma_{\text{thr}}=33$, $p_{\pi\text{-thr}}=4.65$ GeV/c). The choice of CO_2 as radiator gas is being motivated by the low fluorescence probability, required due to the high interaction rates and charged particle flux. The focussing mirror (13 m², focal distance 1.5 m) is divided into two halves above and below the beam pipe, each made of ≈ 40 individual spherical mirror tiles of 6 mm thick SIMAX glass with Al+MgF₂ coating, providing good reflectivity down to 180 nm. The Cherenkov photons are detected using Multianode Photomultiplier Tubes. A wavelength-shifting coating of the PMT window with p-Terphenyl is foreseen to further enhance the UV-sensitivity of the PMTs [2]. Around 20 to 23 detected photons per Cherenkov ring are expected according to simulations and prototype tests, corresponding to N_0 of 130 to 150 cm⁻¹. A detailed technical description of the CBM RICH detector can be found in the Technical Design Report [3], in [4], and in [5]. Here, we focus on two aspects, namely the photon detector R&D, and the development of the electronic readout chain.

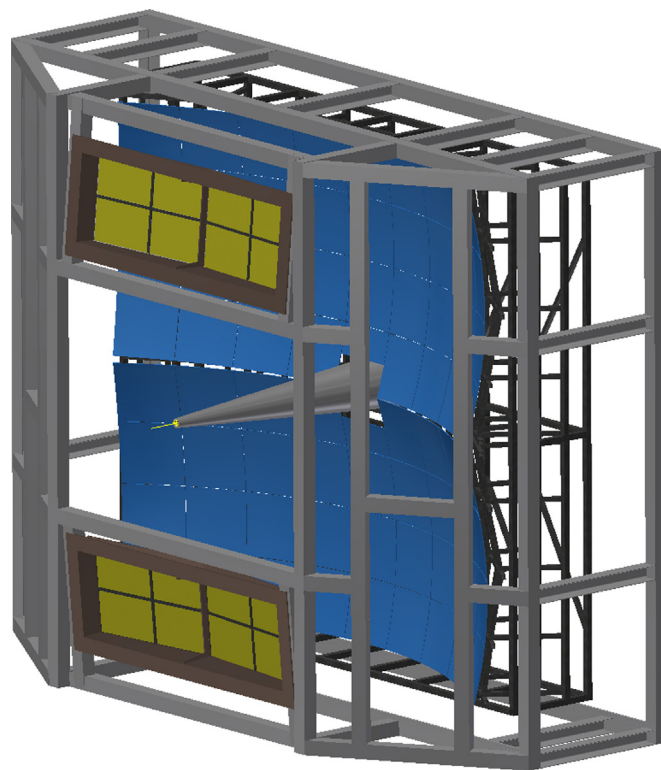


Fig. 2. Sketch of the CBM RICH detector.

3. The CBM RICH photon detector

The CBM RICH photon detector will use Hamamatsu H12700 Multianode Photomultiplier tubes, which were selected following a detailed R&D program on sensor characterization, taking into account also other sensors, among them the Hamamatsu H8500 (64ch, 2×2 inch²), Hamamatsu R11265 (16ch, 1×1 inch²), or the Photonis XP85012 MCP (64ch, 2×2 inch²).

The H12700 MAPMT is based on the Hamamatsu H8500 MAPMT, which served as baseline during the design phase of the CBM RICH detector. It combines the good geometric coverage of the large 2×2 inch² H8500 tube with the single photon optimized dynode system of the smaller R11265 (1×1 inch²). Though only having a Bialkali cathode, the quantum efficiency (and also collection efficiency) could be significantly improved compared to the original H8500, with peak quantum efficiencies regularly exceeding 30%. Furthermore, the spectral response could be slightly shifted towards shorter wavelengths, thus increasing the efficiency in particular in the UV region from 200 nm to 300 nm. Given the $1/\lambda^2$ dependance of the Cherenkov photon yield, this results in a significant increase of Cherenkov photon detection efficiency by up to +30%. A comparison of measured quantum efficiency curves for several H12700 MAPMTs with standard and blue-shifted photocathode is shown in Fig. 3, including a comparison to a typical H8500 MAPMT.

Spatially resolved single-photon efficiency scans have been used to characterize the different MAPMTs. Combining the XY position scan with a fully self-triggered readout chain measuring both amplitude and timing of the PMT signals, nearly all important characteristics (except absolute quantum efficiency) can be derived from a single scan data set, including relative detection efficiency, the sensor dark rate, the amplitude spectrum, the gain, cross talk, or afterpulsing (see [6] for details). By averaging the relative detection efficiency over the active surface, and by using a reference PMT for normalization, a “Single photon efficiency index” can be derived, allowing for a relative comparison of all measured

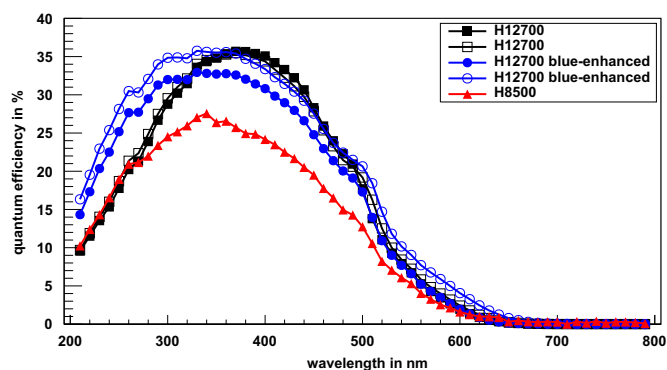


Fig. 3. Comparison of quantum efficiencies for several H8500 and H12700 MAPMTs, some of them with the new blue-shifted photo cathode.

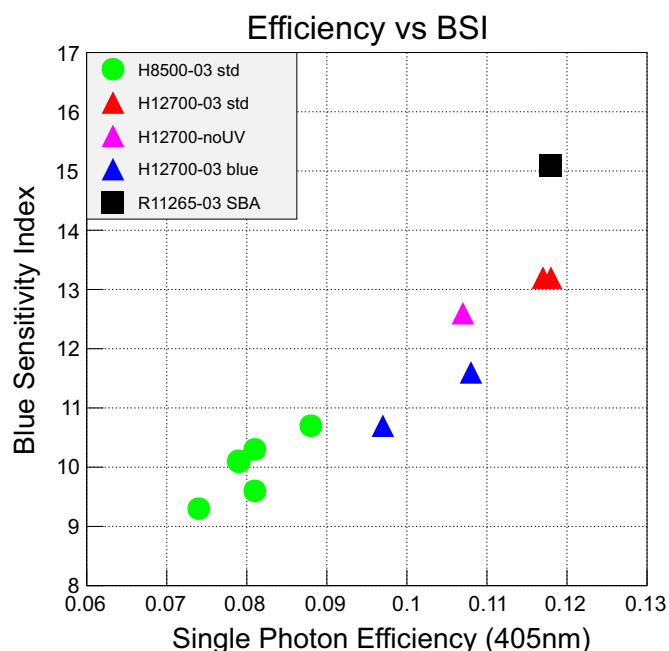


Fig. 4. Correlation between single photon efficiency index from XY scans (X-axis) and Blue Sensitivity Index (Y-axis) as taken from Hamamatsu data sheets.

PMTs in terms of photon detection efficiency at a given wavelength (here 405 nm). This efficiency index can be compared to the “Blue Sensitivity Index”, a measure provided by Hamamatsu and closely related to the quantum efficiency.

Both quantities are closely related, as can be seen in Fig. 4, showing single photon efficiency- and Blue Sensitivity Index for various H8500 and H12700 MAPMTs with and without blue-shifted cathode. Also included for comparison is a single R11265 MAPMT with SBA photo cathode. The new H12700 shows much better performance than the H8500, and, taking additionally into account the better geometrical coverage, nearly competes with the smaller R11265. The H12700 PMTs with blue-shifted cathode are slightly underestimated in this plot due to their shifted peak-efficiency wavelength.

4. Radiation hardness of Hamamatsu H8500/H12700 MAPMTs

An important further aspect in the qualification of a photon sensor for the CBM RICH detector is sufficient radiation hardness with respect to non-ionizing radiation from neutrons, as well as ionizing radiation from photons and charged particles. Detailed

FLUKA simulations predict integrated irradiation doses of up to 10^{12} neq/cm², and up to ≈ 100 Gy ionizing dose in the region of the photon detectors, when assuming a CBM running scenario with 2 months per year of Au+Au collisions at 35 AGeV. Several possible damage scenarios can be imagined, and could be verified or excluded by the measurements:

- The PMTs have a metal housing made of COVAR, an alloy containing 17% of ⁵⁹Co, nickel, and iron. ⁶⁰Co could be produced by neutron capture, which is a beta emitter (0.31 MeV, $\tau=5.7$ y), and might lead to a permanent increase of the PMT darkrate.
- Radiation damage of the photocathode or dynodes could lead to efficiency losses, gain decrease, or increased dark rate.
- Radiation damage to the glass window will cause coloring and loss of transmission.
- The PMT-integrated active voltage divider uses transistor stabilization for the last 3 dynodes. Radiation damage to these transistors could lead to a drift or breakdown of the dynode voltages.
- Fluorescence efficiency or transmission of the WLS coating could degrade.

To approve sufficient radiation hardness of all components, we carried out irradiation tests of several H8500 and H12700 MAPMTs, of PMT glass window samples, WLS-coated quartz substrates, and individual PMT voltage dividers (without the attached PMT). The H8500 and H12700 MAPMTs are considered to be similar enough such that results hold for both types. The voltage dividers were irradiated while under high voltage operation, the dynode voltages were monitored using a data logger.

At the JSI “Jozef Stefan Institute” in Ljubljana, the samples were irradiated at the TRIGA nuclear reactor facility, providing a high flux of thermal neutrons. In the “Strahlenzentrum Giessen”, a ⁶⁰Co source was used to irradiate the samples with energetic gammas of 1.2 MeV/1.3 MeV. It is important to note, that also at the reactor facility, a significant additional ionizing dose (in the order of 10 Gy per 1×10^{12} neq/cm² depending on the operation cycle) is applied due to the radioactive fission products in the fuel elements. Single photon scans of each PMT were carried out before irradiation, after irradiation with neutrons, after subsequent ⁶⁰Co irradiation, and once again after 4 months of “cool-down” time in order to characterize a possible radiation damage.

An important result of these tests is given in Fig. 5, showing the measured dark rate of several PMTs before and after irradiation with different integrated radiation doses. Indeed, a clear increase of darkrate depending on irradiation dose is observed, up to 12 kHz single photon dark rate (sum of all 64 channels) after irradiating with 3×10^{11} neq/cm² plus additional ≈ 150 Gy from the ⁶⁰Co source. However, the last measurement after 4 months of cool down time shows a quick decrease of the darkrate, back close to the original values. This result shows, that activation of long-living nuclides, in particular ⁶⁰Co, plays no significant role. Another important result covers the radiation hardness of the transistor stabilized voltage divider, showing only a minor drift of dynode voltages for irradiation up to $\approx 10^{14}$ neq/cm² (+ 1000 Gy). Only at $\approx 10^{15}$ neq/cm² (+ 10 kGy), a radiation induced breakdown of the stabilization circuit could be observed. The UV glass window samples show only 2% loss of transmission at 200 nm after irradiation with 100 Gy from the ⁶⁰Co source. More severe effects were only observed for much higher integrated doses above ≈ 1000 Gy. The single photon efficiency index for the H12700 MAPMT with the highest integrated dose of 3×10^{11} neq/cm² neutrons plus 145.7 Gy dropped by $\approx 6\%$, which can be partly attributed to the coloring of the glass window. Single photon amplitude spectra measured before and after irradiation showed no significant difference in shape or gain. Fluorescence

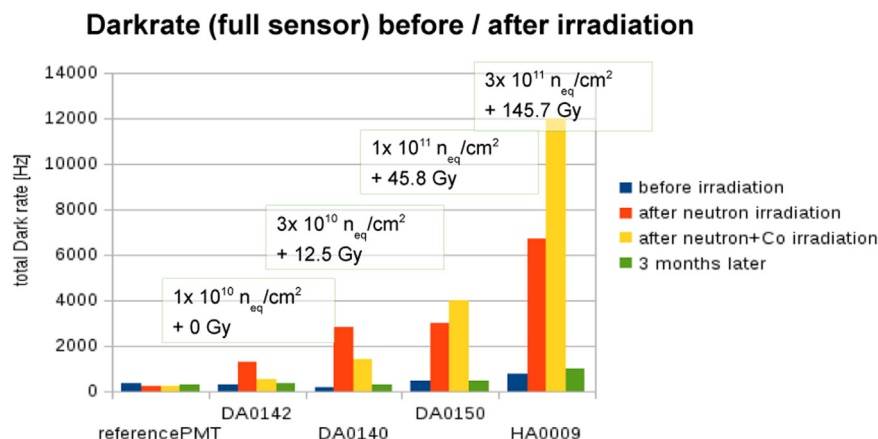


Fig. 5. Dark noise of several H8500 (DA0xxx) and a H12700 (HA0009) MAPMTs before any radiation, after neutron irradiation, and after subsequent ^{60}Co irradiation.

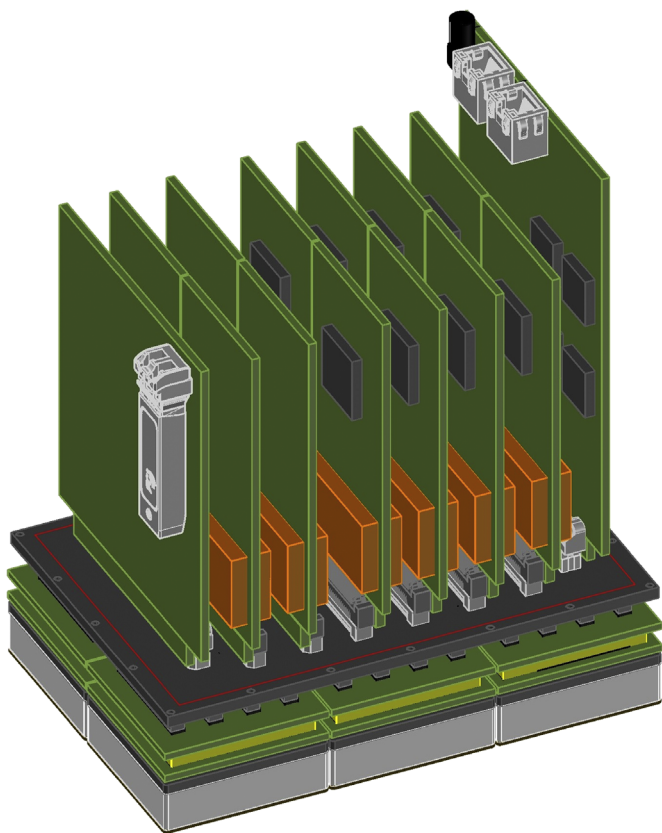


Fig. 6. CBM-RICH readout module for 6 MAPMTs with front-end modules (from left to right): Data Combiner Module, $12 \times$ DIRICH frontend module, and Power Distribution Module.

measurements on the WLS samples showed no significant intensity decrease after irradiation with 100 Gy ionizing dose (Fig. 6).

In summary, no severe problems could be observed with respect to the usage of Hamamatsu H12700 MAPMTs in the CBM RICH photon detector. Following this positive result, 1100 sensors of this type were ordered in summer 2015. Production and delivery of the sensors has started and will continue until mid 2017.

5. The electronic readout chain

The electronic readout chain for the MAPMTs of the photon detector is based on the DIRICH module, a 32 channel

discriminator and FPGA-TDC module being under development. The analog input signals from the PMTs are amplified and then discriminated on the DIRICH module, using the comparators of the differential line receivers of a Lattice ECP5 FPGA. The same FPGA includes a $32+1$ ch FPGA-TDC (tapped delay line technique), digitizing the leading- and trailing edge of the discriminated analog signal to measure both signal arrival time and Time-over-Threshold for amplitude measurement. The aim for leading edge time precision is in the order of the Transit Time spread (TTS) of the MAPMT itself (≈ 300 ps RMS). The new DIRICH module will combine the TDC functionality of the existing HADES “Trigger and readout board” TRB3, and the PADIWA discriminator board [7] on a single module, providing a very economical solution for the sensor readout. The DIRICH is a joint development of the PANDA DIRC, CBM-RICH, and HADES-RICH groups.

The PMTs will be grouped in modules of 6 PMTs sharing a common backplane, with 12 DIRICH modules being plugged in from the back side. A FPGA-based “Data Combiner Module” will combine the digital data from all 12 DIRICH modules to a single optical output link. A “Power Distribution Module” will provide all necessary LV supply lines to the modules, as well as a common HV channel for all six PMTs. The backplane provides all necessary clock- data- and analog connections between PMTs and the modules. It also serves as a gas- and light-tight enclosure of the CO_2 radiator volume, rendering the need for an additional UV transparent glass window.

All electronic modules are currently in the layout phase, first prototypes are expected mid 2016.

Acknowledgments

This work was supported by BMBF Grants 05P12RGFCG, 05P12PXFCE, 05P15PXFCA and 05P15RGFCA, by the GSI F&E-Cooperation with Giessen and Wuppertal (WKAMPE1012), by the Hessian LOEWE initiative through the Helmholtz International Center for FAIR (HIC for FAIR), by the Helmholtz Graduate School for Hadron and Ion Research, by Helmholtz Grant IK-RU-002, by SC ROSATOM through FRRC, and by the Ministry of Education and Science of the Russian Federation (Grant no. 14. A12.31.0002).

References

- [1] B. Friman, et al., (Eds.), The CBM Physics Book: Compressed Baryonic Matter in Laboratory Experiments, in: Springer Series: Lecture Notes in Physics, vol. 814,

- 2011.
- [2] J. Adamczewski-Musch, et al., Nucl. Instrum. Methods A 783 (2015) 43.
- [3] C. Höhne (Ed.) et al., CBM-RICH Technical Design Report, GSI-2014-00528, <http://repository.gsi.de/record/65526>.
- [4] C. Höhne, et al., Nucl. Instrum. Methods A 639 (2011) 294.
- [5] C. Höhne, et al., Nucl. Instrum. Methods A 595 (2008) 187.
- [6] J. Adamczewski-Musch, et al., Nucl. Instrum. Methods A 766 (2014) 101.
- [7] A. Neiser, et al., JINST 8 (2013) C12043.